Applied Clay Science 118 (2015) 221–230

Contents lists available at ScienceDirect

Applied Clay Science

journal homepage: www.elsevier.com/locate/clay

Research paper

Chemical and radiological characterization of Peruíbe Black Mud

Paulo Sergio Cardoso da Silva [a,*], Jefferson Koyaishi Torrecilha [a], Paulo Flávio de Macedo Gouvea [a], Marcelo Francis Máduar [b], Sônia Maria Barros de Oliveira [c], Marcos Antonio Scapin [d]

[a] Research Reactor Center, Energy and Nuclear Research Institute (Instituto de Pesquisas Energéticas e Nucleares), Av. Prof. Lineu Prestes 2242, Cidade Universitária, CEP 05508 000 São Paulo, Brazil
[b] Radiation Metrology Center, Energy and Nuclear Research Institute (Instituto de Pesquisas Energéticas e Nucleares), Av. Prof. Lineu Prestes 2242, Cidade Universitária, CEP 05508 000 São Paulo, Brazil
[c] Institute of Geosciences, University of São Paulo, Rua do Lago 562, 05508-080 São Paulo, Brazil
[d] Chemistry and Environmental Center, Energy and Nuclear Research Institute (Instituto de Pesquisas Energéticas e Nucleares), Av. Prof. Lineu Prestes 2242, Cidade Universitária, CEP 05508 000 São Paulo, Brazil

ARTICLE INFO

Article history:
Received 11 March 2015
Received in revised form 17 September 2015
Accepted 21 September 2015
Available online 22 October 2015

Keywords:
Peruíbe Black Mud
Therapeutic clay
Peloid
Cosmetic clay

ABSTRACT

The Black Mud (PBM) extensively used for therapeutic treatments in the City of Peruíbe, Southwest Brazil, was characterized for its physicochemical properties, chemical constituent and mineralogical composition. Radiometric assay was done by determining its radioactive elements activity concentration and estimating the dose resulting from the mud application on the skin. It was determined that the PBM is a material mainly composed of silt–clayey and sand fine size particles. PBM may be characterized by being enriched in the elements Br, Cr, Sb, Se, and Zn and depleted in Ca, Rb, and Ta, related to the Upper Continental Crust. It has been found that the elements Fe, K, Cl, Mg, Ti, Ca, and P are enriched in the matured form, relative to the *in natura* form during the maturation process. Effective dose assessed for public members indicated that the therapeutic use of the mud poses no radiation risk to the individuals under therapeutic treatment.

1. Introduction

The use of minerals for therapeutic purposes is an ancient practice, particularly with regard to clay minerals such as smectite, kaolinite and palygorskite (López-Galindo and Viseras, 2004; Carretero et al., 2006, Carretero et al., 2013). For a long time, clay has been used in wound healing to relieve skin irritation, with anti-inflammatory purpose, and to treat gastrointestinal disorders. Currently, its use in the pharmaceutical industry is highlighted as an active ingredient as well, due to its high adsorption capacity and specific surface, easy handling in pharmaceutical formulations, as excipient, and also because it promotes drug disintegration, influencing the processes of medicine release, when orally administered. Furthermore, clay is used as topical cosmetics, for its feature of adsorbing substances such as fats and toxins (Churchman et al., 2006). The high number of clay applications is related to its high mineralogical variety, frequency of occurrence and particular properties (López-Galindo and Viseras, 2004). In this context, therapeutic treatments using clay have acquired increasing economic importance.

In therapeutic treatments involving clays, the preferred usage is in its mud form, composed by a mixture of organic and inorganic materials with sea, salt lake or mineral–medicinal water. This mixture is usually called peloid. For the peloid obtainment, the clay remains in contact with water for a long period (about six months), and this process is called maturation (Veniale et al., 2004; Gomes et al., 2013).

In Southeast Brazil, the Black Mud found in Peruíbe city, São Paulo State (Fig. 1), has been extensively used for therapeutic treatments. The material occurs in the plain of Peruíbe city, accumulated in adjacent dikes during overflow events of Preto River, forming the Peruíbe Black Mud (PBM) deposit, which contains approximately 83 thousand tons of mud, with a depth of 75 m. In the city, the mud treatment is done in a therapeutic clinic called "Lamário" and this practice is nowadays sponsored by the Public Health Brazilian System. In the "Lamário", before being matured, the collected mud is sieved, in a 2 mm aperture sieve, in order to separate any courser material, such as stones, leaves and pieces of branches. The maturation is then performed, keeping the mud in contact with sea water, taken 2 km far from the cost, at least for six months in a maturation pond. During this period, the sea water is, periodically, changed twice a month. No agitation is employed in the maturation process. PBM is commonly used for treatment of psoriasis, peripheral dermatitis neuropathy, acne and seborrhea, myalgia, arthritis, and non-articular rheumatic processes. The PBM therapeutic activity and anti-inflammatory efficacy has already been tested, and described by Britschka et al. (2007).

When used for therapeutic or cosmetic purposes clays may not be exempted, *a priori*, of possibly causing adverse health effects. Dangerous minerals for the respiratory system, natural radionuclides and toxic

* Corresponding author.
E-mail address: pscsilva@ipen.br (P.S.C. da Silva).

http://dx.doi.org/10.1016/j.clay.2015.09.016
0169-1317/

Fig. 1. Location of Peruíbe City in Southeast Brazil.

elements may be present, owing to the high specific surface area and ion exchange capability (Cara et al., 2000; Vreca and Dolenec, 2005; Plumlee et al., 2006; López-Galindo et al., 2007; Cantaluppi et al., 2014). No specific regulation has been established yet for mud applications for medicinal purposes. Nevertheless, there is a consensus that clays must have zero or low toxicity (Silva et al., 2011). As a marketed product, every clay-based preparation has to be accompanied by safety information, including an accurate identification of the substance, its main intended or recommended uses, composition and/or information on ingredients, hazards identification, handling and storage, physical and chemical properties, stability and reactivity, and toxicological information (López-Galindo et al., 2007).

The objective of this study was the PBM characterization in its *in-natura* and maturated forms by determining some of its physical-chemical properties, mineralogical and chemical composition, radioactivity content, as well as the assessment of radiation doses arising from the mud application over the human skin during the treatment.

2. Experimental

2.1. Sample identification

For the characterization of the *in natura* mud, five samples were collected from the digs where the mud is in fact being taken for use at the therapeutic clinic. These samples correspond to five different depths within the same cava (samples IN1 to IN5). Other four samples were taken in different locations at the surroundings of that cava (samples IN6 to IN9) to characterize the whole deposit. For the characterization of the matured mud, ten samples (MAT1 to MAT10) were collected at different times directly from the maturation pounds in the "Lamário".

Before the analysis, *in natura* samples were sieved in a 2 mm sieve, following the same procedure adopted in the "Lamário". All the samples were centrifuged to separate and discharge the mud liquid phase excess. Depending on the analytical procedure, wet samples resulting from the centrifugation process were used or a drying procedure at 40 °C was applied.

2.2. Physicochemical characterization

The pH was determined by mixing 10 mL of the wet mud sample with 25 mL of KCl 1.0 mol L^{-1}. The solutions were stirred for 5 min, let to stand for 1 h and, then, the measurement was made. This method was applied to five replicates of one *in natura* and one matured sample. Wet samples were treated, sequentially: a) to determine the percent of moisture content, at 105 °C, for 24 h; b) weight % LOI (loss on ignition) at 450 °C, for 4 h, to estimate the organic matter content and c) the weight % LOI at 1000 °C, for 2 h, to determine the carbonate and hydroxide mass losses by employing an oven furnace and muffle, as needed (Dean, 1974). For the grain size determination, the samples were passed through a set of sieves with 0.425 and 0.075 mm apertures, to determine the amount of fine sand (minor than 0.425 and higher than 0.075 mm) and sand plus clay (minor than 0.075 mm). Swelling power was measured by using water as a polar medium and hexane as a non-polar medium, following the procedure adopted by Foster et al. (1953); the cation exchange capacity (CEC) was determined by the

Table 1
Physical chemical parameters: percentages of silt + clay, sand, moisture, organic matter (O.M.) and LOI at 1000 °C.

	Silt + clay (%)	Sand (%)	Moisture (%)	O.M. (%)[a] LOI at 450 °C	LOI (%)[b] at 1000 °C
IN1	44	46	12	3.6	0.4
IN2	66	32	24	4.0	0.8
IN3	48	46	28	5.4	1.0
IN4	54	43	32	6.0	1.0
IN5	61	33	38	7.1	1.1
IN6	40	57	49	9.7	1.5
IN7	33	67	51	11.0	1.8
IN8	22	73	52	11.8	1.9
IN9	19	77	70	12.0	2.3
Mean	43	53	39	7.8	1.3
S.D.	16	16	18	3.34	0.59
MAT1	31	66	34	5.2	0.8
MAT2	48	46	36	6.6	1.1
MAT3	44	52	38	7.2	1.2
MAT4	53	44	41	8.0	1.2
MAT5	32	67	43	8.2	1.3
MAT6	29	66	43	8.3	1.3
MAT7	32	68	44	8.4	1.3
MAT8	31	65	54	9.7	1.5
MAT9	–	–	64	12.0	2.7
MAT10	–	–	73	20.0	3.0
Mean	38	59	47	9.4	1.5
S.D.[c]	9	10	13	4.2	0.7

[a] Determined by calcination at 450 °C, for 4 h.
[b] Determined by calcination at 1000 °C, for 2 h.
[c] S.D. — standard deviation.

Table 2
Cation exchange capacity (CEC) of selected PBM samples.

Sample	CTC meq/100 g
IN4	33 ± 1
IN5	29 ± 3
MAT1	29.7 ± 0.1
MAT2	26 ± 1

methylene blue titration method (Abayazeed and El-Hinnawi, 2011). For the determination of C/N and H/C ratio, total carbon, hydrogen and nitrogen were determined by using a Perkin Elmer® — CHN 2400 Elemental Analyzer (Perkin Elmer, Inc. Waltham, USA) and the analysis was performed in the Analytical Central Laboratory of the São Paulo University Chemistry Institute.

2.3. X-ray diffractometry

The PBM mineralogical components were identified by X-ray powder diffraction (XRD), using a Siemens automated powder diffractometer, equipped with a graphite monochromator and Cu Kα radiation at 40 kV and 40 mA. All samples were scanned in the 2θ range of 2–60° with a step size of 0.020°, using Cu Kα radiation at 40 kV and 40 mA. Three X-ray patterns were recorded: at air-dried condition, after solvation with ethylene glycol during 24 h and after heating at 550 °C, for 3 h.

2.4. X-ray fluorescence

The chemical characterization was carried out using a wavelength dispersive X-ray fluorescence spectroscopy (WDXRF), with RIGAKU Co. spectrometer, model RIX 3000 with X ray tube, an Rh anode, a 75 μm Be window, a 60 kV maximum acceleration voltage, a scintillation detector NaI(Tl) and a flow-proportional counter. The samples were prepared in pressed pellets, where in 1.8 g of sample, 0.2 g powder wax (analytical grade, HOECHST) was added, mixed and homogenized in Mixer/Mill and, then, the mixture was pressed, using a hydraulic press. The Fundamental Parameters method was applied for correction of the absorption/excitation effects.

2.5. Neutron activation analysis

The elements As, Br, Co, Cr, Cs, Fe, Hf, K, Mg, Mn, Na, Rb, Sb, Sc, Se, Ta, Ti, V, Zn, Zr and rare earth elements (Ce, Eu, La, Lu, Nd, Sm, Tb, and Yb) were determined by the instrumental neutron activation analysis (INAA), in short and long irradiation periods (15 s. and 8 h, respectively). For multi-elemental analysis, approximately, 60 mg and 150 mg of samples and reference materials (Estuarine Sediment, SRM 1646a from NIST and Syenite, Table Mountain, STM-2 from USGS), respectively, were accurately weighed and sealed in pre-cleaned double polyethylene bags for short and long irradiations. Synthetic standards were also prepared by pipetting convenient aliquots of standard solutions (SPEX Certiprep Inc., USA) using Milli-Q water 18.2 MΩ cm^{-1} at 25 °C (Millipore Corporation, USA), onto small filter paper sheets. Samples and reference materials were irradiated in a thermal neutron flux of 10^{12} cm^{-2} s^{-1}, in the IEA-R1 nuclear research reactor at IPEN. Counting time varied from 3 min to 2 h for short and long irradiation, respectively, after the appropriate decay period for each interest nuclide (IAEA, 1990). Gamma spectrometry was performed using a coaxial Be-layer HPGe detector with 22% relative efficiency, 2.09 keV resolution, at 1.33 MeV and associated electronic devices. Spectra were acquired by a multichannel analyzer and analyzed with the aid of spectrum analysis in-house software Vispect2. The methodology evaluations was done cross checking the reference materials and synthetic standards.

2.6. Graphite Furnace Atomic Absorption Spectrometry

For the Cd and Pb determination by Graphite Furnace Atomic Absorption Spectrometry (GFAAS), approximately, 0.30 g of dried samples were dissolved in a microwave closed system with concentrated nitric, hydrochloric, hydrofluoric acids and hydrogen peroxide 30% (Merck, Darmstadt, Germany). The digested samples were allowed to cool at room temperature and diluted with high-purity water.

Measurements were performed by using a Perkin Elmer Analyst 800 graphite furnace atomic absorption spectrometer (Perkin Elmer, Vernon Hills, Illinois, USA). The calibration curves were obtained by diluting certified standard solution (SPEX Certiprep Inc., USA) of the elements of interest to obtain stock solution, further diluted by the AS-800 auto-

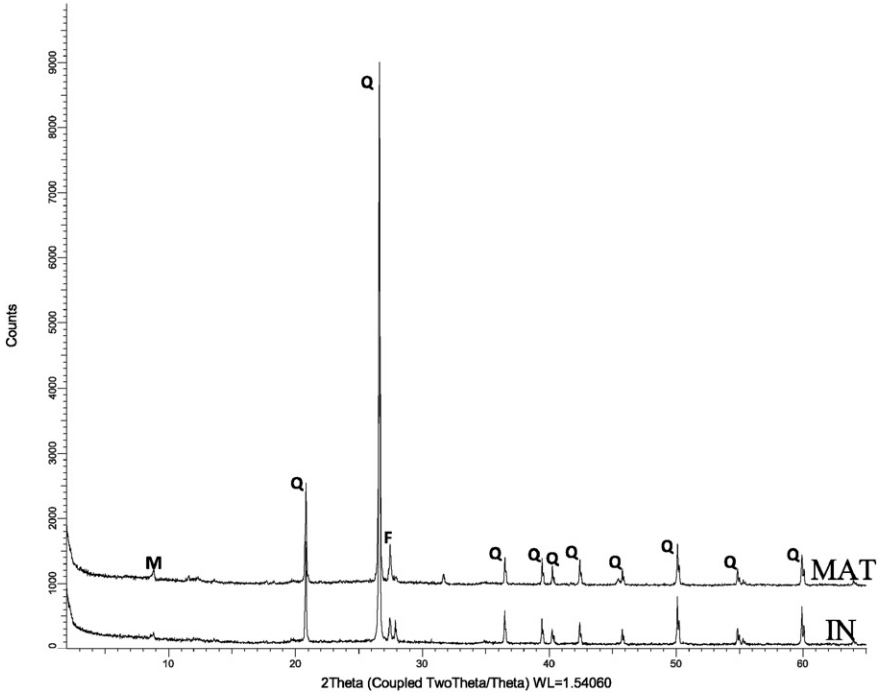

Fig. 2. Diffractogram of the total fraction of PBM *in natura* and matured samples. M = mica, Q = quartz, F = feldspar.

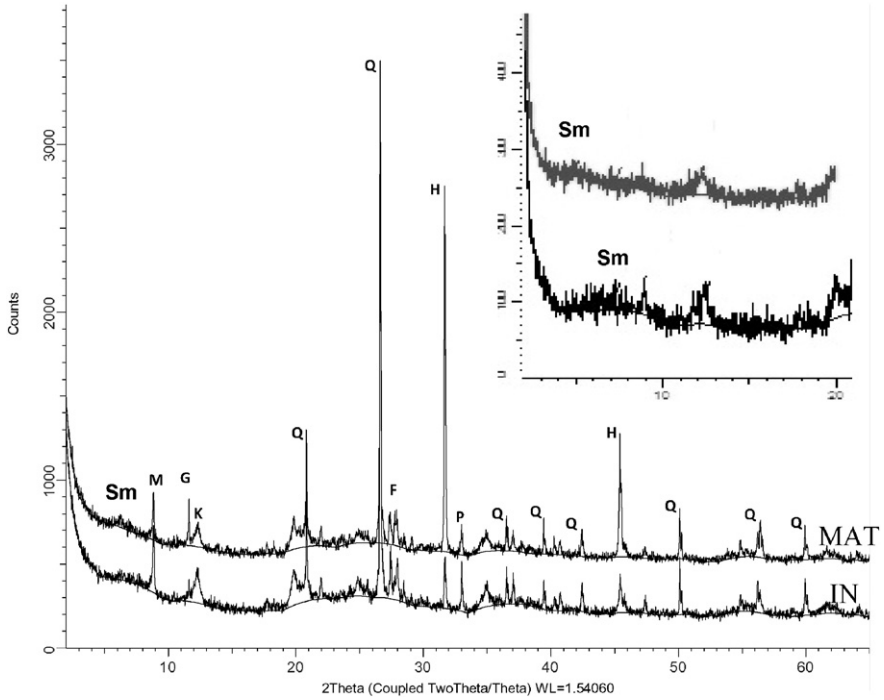

Fig. 3. Diffractogram of the fine fraction (lower than 0.075 mm, silt plus clay) of PBM *in natura* and matured samples. M = mica, Q = quartz, F = feldspar, G = gypsum, k = kaolinite, P = pyrite, H = halite, Sm = smectite. The insert shows the smectite expansion in the glycosylated matured sample.

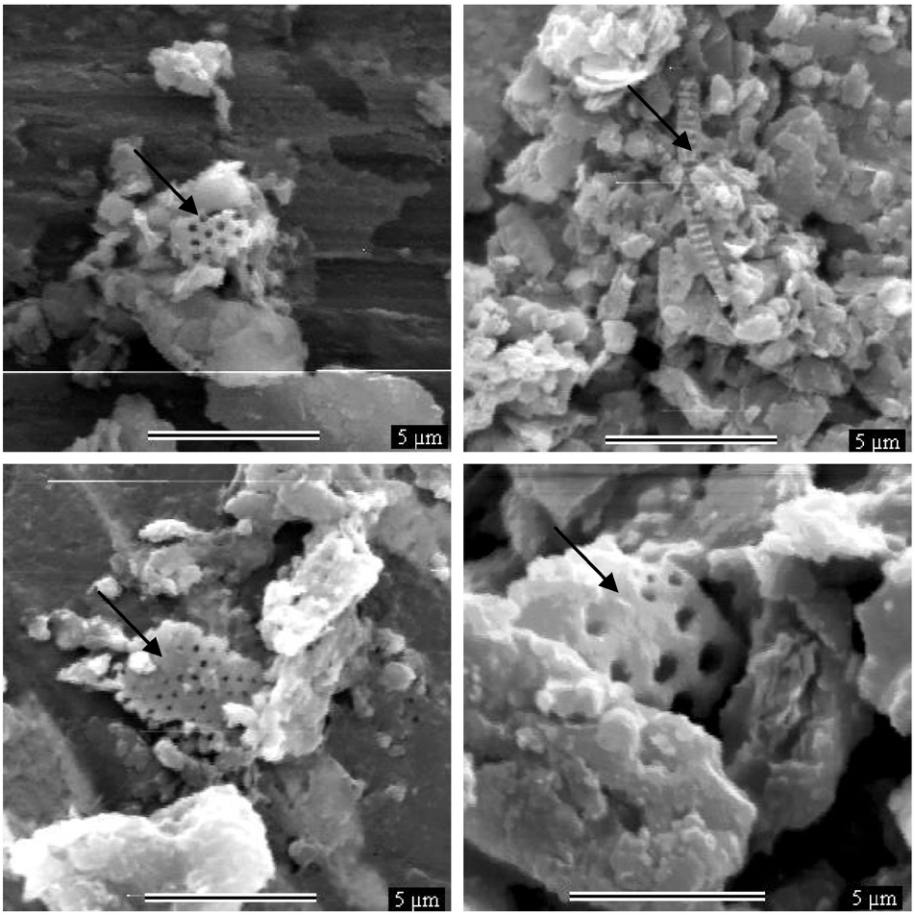

Fig. 4. Micrograph images showing the presence of diatoms in the PBM samples.

sampler. The calibration curve coefficients were obtained by a linear regression fit with least-squares method performed by the spectrometer software. Matrix modifier of $NH_4H_2PO_4$ 0.5% (m/v) and Mg $(NO_3)_2$ 0.03% (m/v) were used to avoid chemical interferences. The blanks were prepared and analyzed by using the same procedure applied to the samples, lowering the detection limit levels. Analyses were carried out in duplicate with differences between the measurements up to 10%. The detection limits for Cd and Pb were determined using the IUPAC criterion (Currie, 2009): the values obtained were 0.016 and 0.85 $mg \cdot kg^{-1}$, respectively.

2.7. Gamma spectrometry

Activity concentrations of ^{226}Ra, ^{228}Ra, ^{210}Pb and ^{40}K were measured by gamma spectrometry with a hyper-pure germanium detector, GEM-15200, from EG&G Ortec. The detector was calibrated with soil, rock and water spiked with radionuclides certified by Amersham. Samples were placed in 100 cm^3 polyethylene flasks, sealed and set apart for about four weeks, prior to the measurements, to ensure reaching of radioactive equilibrium between ^{226}Ra and its short-living decay products. The ^{226}Ra activities were determined by taking the mean activity of three separate photopeaks of its daughter nuclides: ^{214}Pb at 295 keV and 352 keV, and ^{214}Bi at 609 keV. The ^{228}Ra content of the samples was determined by measuring the intensities of the 911 keV and 968 keV gamma-ray peaks from ^{228}Ac. The concentration of ^{210}Pb was determined by measuring the activity of its low energy peak (47 keV). Self-absorption correction was applied because the attenuation for low energy gamma rays is highly dependent upon the sample composition (Cutshall et al., 1983).

3. Results and discussion

3.1. Physicochemical characterization

In most cases, only the fine fraction of clays is marketed for cosmetic and therapeutic purposes. In the case of PBM, application in patients is done with the material in the form it is obtained, after the maturation process. Silt plus clay (less than 0.075 mm) content, showed in Table 1, varied from 19 to 66%, with a mean value of 43% for *in natura* and from 29 to 53%, with a mean value of 38%, for matured samples. The sand content (higher than 0.075 mm) varied from 32 to 77%, with mean value of 53%, for *in natura* and from 46 to 68%, with a mean value of 59%, for matured samples.

The pH of the two representative mud samples was 6.8 and 6.9 for *in natura* and matured ones, respectively, measured in five replicates of each form. Reported values of pH in medicinal mud varies from 6.5 to 8.9 (Karakaya et al., 2010; Knorst-Fouran et al., 2012; Carretero et al., 2014; Muñoz et al., 2015). The pH values may influence the availability of the chemical elements adsorbed in the mineral grains composing the mud and a small change in this parameter may affect ionic exchange properties during skin contact.

The moisture content by mass in the PBM varied from 12 to 70% (Table 1) for *in natura* and from 34 to 73%, for matured mud. The high moisture content found in the black mud is, probably, a consequence of a high number of hydration sites (Banin and Amiel, 1970).

The organic matter content found in medicinal mud may be related to its therapeutic properties and, as described by Gomes et al. (2013), a peloid is constituted by a geological part composed by the clay and water mixture and an organic part that provides biological metabolic activity. Also, according to Pozo et al. (2013), organic matter content is inversely correlated to the abrasiveness of the mud. The content of organic matter in the PBM samples (Table 1) varied from 3.6 to 12%, in the *in natura*, and from 5.2 to 20%, in the matured samples.

Considering the weight % LOI at 1000 °C values (Table 1), which varied from 0.4 to 2.3% for *in natura* and from 0.8 to 3.0% for matured mud, it may be concluded that the PBM presents a low content of coordinated hydroxyl that characterizes clay minerals. Swelling power, measured in one *in natura* and in one matured sample to verify its interaction with a polar and a non-polar medium (water and hexane, respectively) also indicated that both forms of PBM are composed, mainly, by an inert material (sand) (swelling virtually zero) and small amounts of a highly expansible matter with colloidal characteristics, giving a swelling value of 25 and 15 mL, respectively, for *in natura* and matured samples.

The CEC was measured in two *in natura* and two matured samples (Table 2). The obtained results showed a mean value of 30 ± 3 meq/100 g (n = 4) measured for the PBM samples. The low standard deviation indicates that there are no significant differences between *in natura* and matured PBM forms. It is considered that the richness in trace elements, as well as a relatively high water-holding capacity, are important characteristics of medicinal muds and high values of CEC allows the

Table 3
Major elements, in %, in the PBM samples, in literature values and in the Upper Continental Crust, UCC*, values.

	SiO_2	Al_2O_3	SO_3	Na_2O	Fe_2O_3	K_2O	Cl	MgO	TiO_2	CaO	P_2O_5	MnO	LOI[a]
IN1	61 ± 1	17 ± 1	4.9 ± 0.5	4.1 ± 0.4	3.5 ± 0.4	2.1 ± 0.2	1.7 ± 0.2	1.4 ± 0.1	0.5 ± 0.1	0.4 ± 0.1	0.08 ± 0.05	0.04 ± 0.01	4.0
IN2	56 ± 1	15 ± 1	7.3 ± 0.7	1.8 ± 0.2	5.8 ± 0.6	2.8 ± 0.3	2.8 ± 0.3	2.3 ± 0.2	0.8 ± 0.1	0.6 ± 0.1	0.12 ± 0.05	0.06 ± 0.01	4.8
IN3	53 ± 1	15 ± 1	7.6 ± 0.8	2.7 ± 0.3	6.1 ± 0.6	2.6 ± 0.3	3.6 ± 0.4	2.5 ± 0.2	0.9 ± 0.1	0.6 ± 0.1	0.18 ± 0.05	0.06 ± 0.01	6.3
IN4	54 ± 1	14 ± 1	8.1 ± 0.8	2.3 ± 0.2	6.0 ± 0.6	2.4 ± 0.2	2.7 ± 0.3	2.2 ± 0.2	0.8 ± 0.1	0.6 ± 0.1	0.15 ± 0.05	0.05 ± 0.01	7.0
IN5	53 ± 1	16 ± 1	5.8 ± 0.6	2.0 ± 0.2	6.6 ± 0.7	2.1 ± 0.2	1.4 ± 0.1	4.4 ± 0.4	0.8 ± 0.1	0.4 ± 0.1	0.13 ± 0.05	0.06 ± 0.01	8.2
IN6	51 ± 1	17 ± 1	5.0 ± 0.5	2.1 ± 0.2	6.1 ± 0.6	2.1 ± 0.2	1.4 ± 0.1	4.5 ± 0.4	0.8 ± 0.1	0.7 ± 0.1	0.12 ± 0.05	0.05 ± 0.01	11.2
IN7	50 ± 1	15 ± 1	5.8 ± 0.6	2.7 ± 0.3	5.6 ± 0.6	2.0 ± 0.2	1.6 ± 0.2	4.4 ± 0.4	0.8 ± 0.1	1.0 ± 0.1	0.13 ± 0.05	0.05 ± 0.01	12.7
IN8	50 ± 1	16 ± 1	5.9 ± 0.6	2.3 ± 0.2	5.9 ± 0.6	2.1 ± 0.2	1.4 ± 0.1	3.6 ± 0.4	0.8 ± 0.1	0.5 ± 0.1	0.13 ± 0.05	0.02 ± 0.01	13.7
IN9	54 ± 1	14 ± 1	5.3 ± 0.5	1.9 ± 0.2	4.4 ± 0.4	3.1 ± 0.3	2.0 ± 0.2	1.6 ± 0.2	1.0 ± 0.1	0.6 ± 0.1	0.18 ± 0.05	0.02 ± 0.01	14.3
MAT1	54 ± 1	14 ± 1	7.8 ± 0.8	2.6 ± 0.3	5.9 ± 0.6	2.5 ± 0.3	3.8 ± 0.4	2.2 ± 0.2	0.8 ± 0.1	0.6 ± 0.1	0.18 ± 0.05	0.06 ± 0.01	6.0
MAT2	49 ± 1	15 ± 1	6.0 ± 0.6	3.3 ± 0.3	5.4 ± 0.5	2.1 ± 0.2	4.0 ± 0.4	6.5 ± 0.7	0.8 ± 0.1	0.6 ± 0.1	0.12 ± 0.05	0.05 ± 0.01	7.7
MAT3	57 ± 1	14 ± 1	6.0 ± 0.6	2.1 ± 0.2	5.0 ± 0.5	1.9 ± 0.2	1.7 ± 0.2	3.8 ± 0.4	0.7 ± 0.1	0.5 ± 0.1	0.12 ± 0.05	0.04 ± 0.01	8.4
MAT4	50 ± 1	16 ± 1	5.5 ± 0.6	2.9 ± 0.3	6.1 ± 0.6	2.0 ± 0.2	2.8 ± 0.3	5.1 ± 0.5	0.8 ± 0.1	0.6 ± 0.1	0.11 ± 0.05	0.06 ± 0.01	9.2
MAT5	50 ± 1	15 ± 1	5.8 ± 0.6	3.0 ± 0.3	5.9 ± 0.6	2.1 ± 0.2	2.9 ± 0.3	5.1 ± 0.5	0.8 ± 0.1	0.7 ± 0.1	0.14 ± 0.05	0.05 ± 0.01	9.5
MAT6	45 ± 1	14 ± 1	5.4 ± 0.5	6.3 ± 0.6	5.2 ± 0.5	1.9 ± 0.2	6.1 ± 0.6	5.7 ± 0.6	0.7 ± 0.1	0.7 ± 0.1	0.13 ± 0.05	0.08 ± 0.01	9.6
MAT7	58 ± 1	13 ± 1	6.1 ± 0.6	2.0 ± 0.2	3.9 ± 0.4	2.5 ± 0.3	2.2 ± 0.2	2.2 ± 0.2	0.7 ± 0.1	0.5 ± 0.1	0.15 ± 0.05	0.03 ± 0.01	9.7
MAT8	59 ± 1	12 ± 1	5.6 ± 0.6	2.1 ± 0.2	3.3 ± 0.3	2.4 ± 0.2	2.1 ± 0.2	2.0 ± 0.2	0.6 ± 0.1	0.5 ± 0.1	0.14 ± 0.05	0.03 ± 0.01	11.2
MAT9	55 ± 1	13 ± 1	6.0 ± 0.6	2.2 ± 0.2	4.2 ± 0.4	2.4 ± 0.2	2.1 ± 0.2	2.1 ± 0.2	0.7 ± 0.1	0.5 ± 0.1	0.14 ± 0.05	0.03 ± 0.01	14.7
MAT10	53 ± 1	12 ± 1	3.7 ± 0.4	2.5 ± 0.3	1.6 ± 0.2	1.2 ± 1.2	3.6 ± 0.4	0.5 ± 0.1	0.3 ± 0.1	0.09 ± 0.01	0.02 ± 0.01	0.02 ± 0.01	23
Quintela et al. (2012)	16–63	3.6–20	0.06–4.8	0.15–4.3	1.7–7.3	0.4–3.2	–	0.3–22	0.2–1.2	0.2–27	0.06–0.2	0.01–0.6	6.9–54
Sánchez-Espejo et al., (2014)	34–57	11–19	–	0.6–3.1	3.4–9.3	1.2–2.4	–	2.0–13	0.4–1.4	1.0–20	0.10–0.29	0.03–0.18	7.1–22
UCC*	66	15.2	–	3.89	4.49	3.39	–	2.20	0.5	4.19	0.20	0.07	–

[a] Sum of the weight % loss at 450 and 1000 °C.

Table 4
Trace elements, in μg g^{-1}, except Cd in ng g^{-1}, in PBM samples compared to the Upper Continental Crust, UCC Taylor and McLennan (1991), threshold effect concentration (TEC) and probable effect concentration (PEC) (MacDonald et al., 2000).

	As	Ba	Br	Cd[a]	Ce	Co	Cr	Cs	Eu	Hf	La	Lu	Nd
IN1	7.3 ± 0.7	357 ± 20	95.7 ± 0.6	330 ± 10	63 ± 3	8.7 ± 0.7	51 ± 3	4.2 ± 0.2	1.1 ± 0.1	4.5 ± 0.1	31 ± 1	0.27 ± 0.02	22 ± 3
IN2	5.5 ± 0.6	212 ± 13	66.3 ± 0.4	30.2 ± 0.2	39 ± 2	5.4 ± 0.4	32 ± 2	2.8 ± 0.2	0.75 ± 0.07	2.7 ± 0.1	19.8 ± 0.9	0.16 ± 0.01	17 ± 3
IN3	12.2 ± 1.1	432 ± 24	169.8 ± 1	33 ± 2	76 ± 4	10.1 ± 0.7	62 ± 4	4.8 ± 0.3	1.4 ± 0.1	4.4 ± 0.1	37 ± 2	0.29 ± 0.02	31 ± 5
IN4	9.6 ± 0.4	335 ± 88	97.6 ± 0.6	3.1 ± 0. 6	53 ± 2	8.1 ± 0.1	52 ± 1	3.8 ± 0.2	0.96 ± 0.02	2.2 ± 0	27 ± 0.5	0.26 ± 0.01	31 ± 3
IN5	7.8 ± 0.4	338 ± 90	92.1 ± 0.6	15 ± 4	50 ± 2	7.8 ± 0.1	49 ± 1	3.3 ± 0.2	0.9 ± 0.02	3.4 ± 0	24.6 ± 0.4	0.22 ± 0.01	23 ± 2
IN6	17.1 ± 1.2	621 ± 104	ND	230 ± 20	89 ± 4	15 ± 0.3	90 ± 5	8 ± 0.9	1.56 ± 0.09	5.6 ± 0.1	42 ± 1	0.33 ± 0.03	41 ± 2
IN7	13.5 ± 1	540 ± 83	ND	319 ± 5	78 ± 4	11.8 ± 0.3	82 ± 5	5.7 ± 0.7	1.23 ± 0.07	7.6 ± 0.2	38 ± 1	0.31 ± 0.03	37 ± 1
IN8	16.7 ± 1.2	550 ± 91	ND	290 ± 6	84 ± 4	12.2 ± 0.3	83 ± 5	6.7 ± 0.7	1.28 ± 0.07	14.3 ± 0.3	42 ± 1	0.35 ± 0.03	40 ± 3
IN9	8.6 ± 0.7	721 ± 121	ND	25.3 ± 0.7	53 ± 2	5.4 ± 0.1	67 ± 4	5.1 ± 0.6	0.82 ± 0.05	13.1 ± 0.3	26.8 ± 0.7	0.25 ± 0.02	24 ± 2
MAT1	7.6 ± 0.4	427 ± 113	136.3 ± 0.8	21 ± 6	49 ± 2	7.5 ± 0.1	50 ± 1	3.6 ± 0.2	0.89 ± 0.02	3.3 ± 0	25 ± 0.4	0.22 ± 0.01	24 ± 2
MAT2	7.1 ± 0.3	363 ± 96	127.1 ± 0.6	34 ± 1	52 ± 2	8 ± 0.1	51 ± 1	3.6 ± 0.2	0.89 ± 0.02	3.2 ± 0	22.9 ± 0.4	0.21 ± 0.01	22 ± 2
MAT3	10 ± 0.9	297 ± 19	88.1 ± 0.5	7 ± 4	56 ± 3	7.7 ± 0.6	47 ± 3	3.6 ± 0.2	1.14 ± 0.11	3.9 ± 0.1	30 ± 1	0.23 ± 0.01	28 ± 4
MAT4	11.7 ± 0.9	459 ± 77	ND	39.0 ± 0.6	76 ± 4	12.5 ± 0.3	72 ± 4	6.2 ± 0.7	1.15 ± 0.07	4.9 ± 0.1	36 ± 1	0.28 ± 0.02	34 ± 1
MAT5	12.2 ± 0.9	476 ± 81	ND	268 ± 8	82 ± 4	12.7 ± 0.3	83 ± 5	6.9 ± 0.8	1.36 ± 0.08	6.1 ± 0.1	40 ± 1	0.31 ± 0.03	35 ± 1
MAT6	10.9 ± 0.8	429 ± 67	ND	273 ± 6	67 ± 3	6.8 ± 0.2	71 ± 4	6 ± 0.7	1.14 ± 0.07	4.4 ± 0.1	32.2 ± 0.9	0.24 ± 0.02	30 ± 1
MAT7	10.3 ± 0.5	384 ± 51	162.6 ± 1.2	46.1 ± 0.3	68 ± 2	10.2 ± 0.1	72 ± 3	4.6 ± 0.2	1.28 ± 0.05	5 ± 0.1	35.1 ± 0.9	0.26 ± 0.03	51 ± 12
MAT8	10.7 ± 0.5	409 ± 53	110.3 ± 0.9	490 ± 30	67 ± 2	9.4 ± 0.2	81 ± 3	4.3 ± 0.2	1.36 ± 0.03	6.5 ± 0.1	34.2 ± 0.6	0.34 ± 0.03	30 ± 1
MAT9	11 ± 0.6	353 ± 39	172.1 ± 1.3	41.080 ± 0.002	71 ± 2	11.1 ± 0.2	74 ± 3	5.2 ± 0.3	1.49 ± 0.03	5.2 ± 0.1	35.5 ± 0.6	0.32 ± 0.03	45 ± 10
MAT10	10.2 ± 0.5	345 ± 49	162.7 ± 1.2	61 ±	75 ± 2	12.2 ± 0.2	81 ± 3	5.4 ± 0.3	1.51 ± 0.03	5.6 ± 0.1	38.2 ± 0.7	0.32 ± 0.03	39 ± 11
UCC	1.5	550	2.1	100	64	10	35	3.7	0.88	5.8	30	0.38	26
TEC/PEC	9.79/33			0.99/4.98			44.3/111						

mud to trap a higher quantity of these elements (Karakaya et al., 2010). Compared to other clay minerals, commonly used for therapeutic or cosmetic purposes, PBM has higher CEC than kaolinite, but, lower than that of smectite. Quintela et al. (2012) reports CEC varying from 10 to 30 for peloids from Portugal, Italy and Spain.

The X-ray diffraction pattern of the bulk mud powered and sieved to less than 0.075 mm, showed in Fig. 2, confirms that the PBM is composed, basically, by quartz with small amounts of muscovite and feldspar. Besides, no difference was observed between *in natura* and matured mud, mainly because the diffractogram is completely dominated by the quartz signal. A diffractogram obtained with the fraction lower than 0.075 mm, separated from the bulk sample by sieving, is showed in Fig. 3. In this case, it is possible to verify that small amounts of gypsum, kaolinite, pyrite and halite are, also, present in the PBM composition. A small 001 peak of smectite also appears in the diffractogram pattern and, in the glycosylated diffractogram (showed in the insert of Fig. 3 for the matured sample) the peak migrates to around 17 Å. Although present in small amount, smectite may also contribute to the therapeutic activity of the PBM since this clay mineral is generally found in medicinal peloids (Fernández-González et al., 2013; Pozo et al., 2013). As the same, it is noted that the peaks of gypsum and halite are more prominent in matured than in *in natura* PBM form, probably due to precipitation occurring with sea water interaction, during the maturation processes. This process has, already, been previously reported by other authors, comparing the composition of peloids before and after the maturation processes (Veniale et al., 2004; Carretero et al., 2007; Carretero et al., 2010; Tateo et al., 2010).

Besides the great amount of silica detected by X-Ray diffraction, electronic microscopy revealed the diatom presence, as showed in Fig. 4, what contributes to the with amorphous silica content.

3.2. Elemental characterization

The concentrations of major elements, measured by WDXRF, are given in Table 3. The large variability observed in mineralogical and chemical medicinal mud constitution is certainly related to its geological origin; typically, the amount of major elements varies in wide ranges (Quintela et al., 2012; Sánchez-Espejo et al., 2014). It is possible to note that for major elements, quartz is the main constituent of this mud and, compared with literature values (Table 3), it may be observed that PBM is depleted in Ca, Mg and Mn and enriched in SO_3. Compared to the Upper Continental Crust, UCC, (Taylor and McLennan, 1991), PBM is depleted in Ca.

It is, also, worth noting that PBM contains high amounts of sulfur. Considering that the diffractogram of the fine fraction only shows trace amounts of iron bearing minerals, probably most of the iron present must be in an amorphous form in the mud, such as iron oxyhydroxide.

Comparing in *natura* and matured mud, as to the content of major elements, it is verified that Cl and Mg elements tend to be enriched in the matured form. One hypothesis for this enrichment is the precipitation of halite and gypsum observed in the diffractogram of Fig. 3.

The concentration of trace elements is showed in Table 4, for those elements determined by INAA and GFAAS. To be used as therapeutic and cosmetic products, clays, in general, have to be completely characterized as for the impurity content, such as trace elements.

As there is no established official regulations about chemical composition for peloids, both as raw material and matured form, to be used in pelotherapy, the obtained results for PBM were compared to consensus-based sediment quality guidelines (SQGs), also showed in Table 4, defined by MacDonald et al. (2000). The SQG values, such as the threshold effect concentration (TEC) and probable effect concentration (PEC) provide a reliable basis for assessing sediment quality conditions in aquatic ecosystems.

The comparison of PBM concentrations with the SQG values revealed that As and Cr, in most of the samples and Zn, in two matured samples, are above the TEC and none of them is higher than PEC. Compared with the values for these elements presented by Quintela et al. (2012) for several peloids found in European spas, PBM concentrations are in the same range.

Few quantitative studies on absorption of these potentially toxic elements in humans, after dermal exposure, were found. Absorption of Cd compounds through the skin is considered negligible (Nordberg et al., 2007); arsenic measured in Rhesus monkeys (Wester et al., 1993) indicates less than 7% of absorption, after 24 h. Skin exposure to inorganic lead has shown that the absorption was only 0.06% during 1 month exposure to soluble inorganic salt of this metal (Stauber et al., 1994). However, some exposure may occur from cosmetics (Al-Ashban et al., 2004).

Although occurring, the skin absorption of V, Se and Co can, also, be considered negligible, as shown by animal studies (Medinsky et al., 1981; Roshchin et al., 1982; Filon et al., 2004).

Pb	Rb	Sb	Sc	Se	Sm	Ta	Tb	Th	U	V	Yb	Zn	Zr
21.45 ± 0.004	67 ± 3	0.4 ± 0.07	11.8 ± 0.5	1.6 ± 0.5	4.9 ± 0.3	0.78 ± 0.06	0.6 ± 0.09	8.4 ± 0.8	2.4 ± 0.2	38 ± 5	1.5 ± 0.2	82 ± 3	208 ± 19
14 ± 1	44 ± 2	0.41 ± 0.06	7.4 ± 0.3	1.2 ± 0.4	3.1 ± 0.2	0.53 ± 0.04	0.3 ± 0.03	5.1 ± 0.5	1.6 ± 0.1	41 ± 5	1 ± 0.1	37 ± 2	
13.65 ± 0.06	82 ± 4	0.81 ± 0.1	13.5 ± 0.6	ND	5.9 ± 0.3	0.76 ± 0.07	0.56 ± 0.09	9.7 ± 1	3.4 ± 0.2	ND	1.7 ± 0.2	92 ± 4	216 ± 26
20.2 ± 0.9	59 ± 2	1.01 ± 0.04	8.9 ± 0.04	0.17 ± 0.04	4.3 ± 0.2	0.55 ± 0.03	0.63 ± 0.02	8.4 ± 0.4	2.5 ± 0.1	82 ± 8	1.6 ± 0.1	91 ± 3	171 ± 9
25.05 ± 0.04	13 ± 1	1.1 ± 0.1	8.53 ± 0.04	ND	3.9 ± 0.2	0.46 ± 0.04	0.42 ± 0.04	7.6 ± 0.4	2.8 ± 0.1	77 ± 5	1.2 ± 0.1	154 ± 6	100 ± 17
17.77 ± 0.04	106 ± 5	0.54 ± 0.1	16.3 ± 0.1	ND	6.7 ± 0.5	1 ± 0.1	0.61 ± 0.13	13 ± 1	5.2 ± 0.3	107 ± 13	2.1 ± 0.3	80 ± 4	350 ± 40
20.74 ± 0.03	80 ± 4	0.5 ± 0.09	12.6 ± 0.1	ND	6 ± 0.5	0.91 ± 0.09	0.66 ± 0.12	12 ± 1	4.4 ± 0.3	88 ± 9	2 ± 0.3	75 ± 4	389 ± 43
20.51 ± 0.05	98 ± 5	0.6 ± 0.1	13.3 ± 0.1	1 ± 0.4	6.1 ± 0.5	0.99 ± 0.1	0.62 ± 0.07	13 ± 1	5.9 ± 0.4	81 ± 5	1.9 ± 0.3	71 ± 4	407 ± 116
16.08 ± 0.01	88 ± 4	0.6 ± 0.1	9.23 ± 0.09	0.2 ± 0.2	4.1 ± 0.3	0.99 ± 0.09	0.47 ± 0.11	8.9 ± 0.7	5 ± 0.3	55 ± 5	1.6 ± 0.3	43 ± 2	548 ± 45
12.37 ± 0.02	56 ± 2	ND	8.44 ± 0.04	ND	3.8 ± 0.2	0.54 ± 0.05	0.48 ± 0.04	7.3 ± 0.4	2.3 ± 0.2	50 ± 9	1.3 ± 0.1	87 ± 3	132 ± 25
23.2 ± 0.2	64 ± 2	0.9 ± 0.1	8.88 ± 0.04	0.13 ± 0.05	3.6 ± 0.1	0.61 ± 0.05	0.43 ± 0.04	7.5 ± 0.4	2.4 ± 0.1	33 ± 6	1.3 ± 0.1	95 ± 4	142 ± 18
30.8 ± 0.2	64 ± 3	0.65 ± 0.06	10.6 ± 0.4	1.9 ± 0.3	5 ± 0.3	0.74 ± 0.05	0.47 ± 0.06	7.5 ± 0.7	3.4 ± 0.2	ND	1.3 ± 0.2	74 ± 3	192 ± 17
26.9 ± 0.8	72 ± 4	0.49 ± 0.1	13.4 ± 0.1	ND	5.5 ± 0.4	0.88 ± 0.05	0.59 ± 0.08	10.1 ± 0.9	4 ± 0.3	102 ± 13	1.8 ± 0.3	71 ± 4	240 ± 20
22.5 ± 0.4	89 ± 4	0.5 ± 0.1	14 ± 0.1	ND	6.2 ± 0.5	0.84 ± 0.09	0.7 ± 0.1	11.2 ± 0.9	4.5 ± 0.3	54 ± 6	1.7 ± 0.3	78 ± 4	388 ± 31
14.03 ± 0.02	74 ± 4	0.5 ± 0.1	11.7 ± 0.1	ND	5 ± 0.4	0.9 ± 0.1	0.5 ± 0.1	9.2 ± 0.8	4 ± 0.3	86 ± 11	1.7 ± 0.3	67 ± 4	243 ± 36
13.8 ± 0.2	41 ± 2	0.8 ± 0.1	11.3 ± 0.1	2 ± 5	5.7 ± 0.2	0.67 ± 0.04	0.67 ± 0.09	10.4 ± 0.6	3.2 ± 0.2	69 ± 7	1.4 ± 0.1	96 ± 5	251 ± 108
20.1 ± 0.1	76 ± 3	0.7 ± 0.1	11.7 ± 0.1	ND	5.6 ± 0.2	0.8 ± 0.1	0.3 ± 0.2	9.7 ± 0.5	4.8 ± 0.3	71 ± 7	2.1 ± 0.1	92 ± 5	301 ± 112
21.2 ± 0.2	82 ± 4	0.8 ± 0.1	12.6 ± 0.1	ND	5.9 ± 0.2	0.5 ± 0.2	0.8 ± 0.1	10 ± 0.6	3.5 ± 0.3	94 ± 8	2.1 ± 0.2	123 ± 6	309 ± 43
16.5 ± 0.1	79 ± 3	1.1 ± 0.2	13.1 ± 0.1	ND	6.2 ± 0.2	0.93 ± 0.07	0.4 ± 0.1	10.9 ± 0.6	3.5 ± 0.3	72 ± 18	1.8 ± 0.1	129 ± 6	467 ± 87
20	110	0.2	14	0.05	4.5	2.2	0.64	11	2.8	60	2.2	71	190
35.8/128												121/459	

3.3. Geochemistry

Geochemically, in comparison with the UCC, it can be seen that PBM is enriched in As, Br, Cr, Sb, Se, Zn and Zr (Table 4). Nevertheless, the values observed for As, Cr, Sb, and Zn are in good agreement with the data presented by Silva et al. (2011) for the fine fraction of the sediment found in the region, indicating that this enrichment is linked to the surrounding lithology. The same can be observed for the elements Rb and Ta, which are depleted related to the UCC, but, in agreement with the local lithology concerning these elements.

Figs. 5 and 6 show the cluster analysis (CA) and the principal component analysis (PCA) results applied to the concentrations obtained for the PBM samples. PCA is a multivariate technique that quantifies the significant variation in a data set, reducing the number of variables to a small number of indices, retaining a maximum amount of the variance (Einax et al., 1997; Gemperline, 2006) and resulting in the retention of only the important characteristics of the original data; cluster analysis is a multivariate technique whose primary purpose is to assemble objects into groups, or clusters, exhibiting high internal similarity and high external dissimilarity (Einax et al., 1997). According to the PCA analysis, higher loadings were obtained for the elements As, Br, Ca, Cd, Co, Cr, Cs, Fe, Mg, Sc, Rb, Ta, Th, U, V and REE (Factor 1, Fig. 6), representing the lithological input in the area and contributing with approximately 44% of the observed variance; they are mainly grouped together in the group 2d of cluster analysis (Fig. 5). The second most contributing factor to the observed variance is the presence of high loading factors for elements such as Ba, Hf, K and Zr with, approximately, 12% of the observed variance (Factor 2, Fig. 6), and are grouped together in group 2c (Fig. 5). Cluster analysis results (Fig. 5), also, highlight the similarity among the elements Pb, Zn, Sb, Mn and Si (group 1b, Fig. 5) and among the elements P, S, Ti and Al (group 1a, Fig. 5).

Considering PCA results, factors 1 and 2 account for 56% of the observed variance. The remaining factors (Factors 3 to 5, Fig. 6) account, together, for 22% of the explained variance, indicating that the elements forming these factors must be related to mineral phases showing less variability and linked to the mineral forming elements Si and Al. Similar results can be observed in the cluster analysis, in which the elements forming group 1 (Fig. 5) must, probably, be related to the structural composition of the minerals forming the mud, although representing different mineral phases, since the elements Si and Al are classified in different groups. This fact must be related to the predominant amount of quartz over the aluminosilicates. On the other hand, the elements forming group 2 must, probably, be related to non-structural mud phases, such as iron oxyhydroxides and organic matter.

The elemental ratio between C, N and H is, generally, used to assess the origin of organic matter in sediments. While organic matter derived from marine phytoplankton presents C/N ratio ranging from 4.0 to 10.0 and H/C higher than 1.7, the values derived from terrestrial environment are, generally, higher than 20.0 and lower than 1.3, respectively (Talbot and Livingstone, 1989; Meyers, 2003; Wilson et al., 2005). Table 5 shows the C, N and H percentages, as well as the C/N and H/C ratios in the PBM samples. The C/N and H/C elemental ratios found indicate, therefore, that the PBM organic matter is mainly derived from terrestrial plants. The peloid deposit, therefore, was formed by the interaction of the marine sediment deposition (evidenced by the diatom presence, Fig. 4) and the estuary vegetation.

The mean value of the organic matter to total carbon (OM:C) ratio was 2.15. Nevertheless, four out of the 19 samples presented this ratio significantly higher than the mean value (samples MAT 7–10). Although not clear, possible explanations for this fact can be the dehydroxylation of some minerals below 450 °C of temperature (Jang et al., 2014), loss of Fe-sulfide minerals or different clay minerals assemble in those samples.

3.4. Radiological characterization

Another concern about using mineral clay for therapy treatments is its radioactivity content due to natural radionuclides, normally, associated with the clays (Nikolov et al., 2012; Ramasamy et al., 2014). The activity concentrations obtained for ^{226}Ra, ^{228}Ra, ^{210}Pb, and ^{40}K in the PBM samples are presented on Table 6. Compared to the average worldwide soil activity concentrations (UNSCEAR, 2010), the concentrations obtained were, generally, lower than the reported values.

Radiological implications of using the PBM in topical applications were evaluated by performing a modeling in which a deterministic computer code was used to calculate the absorbed dose to the skin, from the activity concentrations and exposure geometry, VARSKIN 3 (Durham, 2006). Very conservative assumptions were adopted, in which, hypothetical mud, containing simultaneously radionuclide concentrations above the maximum experimental concentrations of ^{226}Ra, ^{228}Ra, ^{210}Pb and ^{40}K determined in the samples, was applied to the

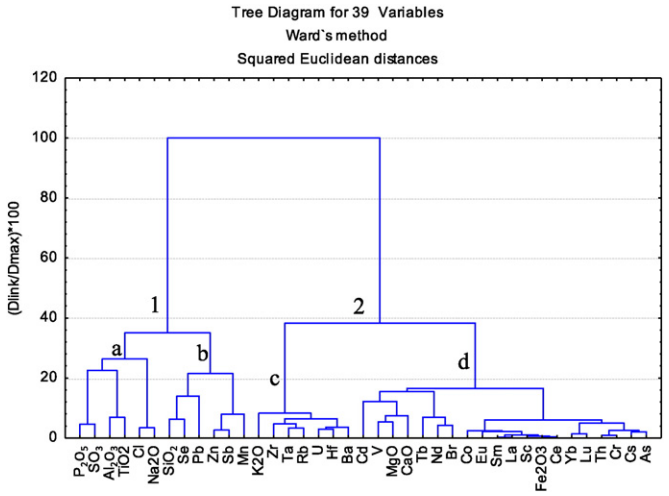

Fig. 5. Dendrogram obtained for the elemental pattern in the PBM samples.

code. Mud application is modeled as a 2-dimensional source disk, directly placed on the skin. The input parameters for VARSKIN 3 are shown in Table 7.

For the assessment, two scenarios were considered, by applying the respective input set to each one:

- Scenario 1: The parameters simulate 1 kg of the hypothetical mud distributed in a 2-D disk with an area of 20,000 cm^2, corresponding to the total body surface area of a male adult (ICRP, 2007). This is the situation when the mud is applied over large portions of the patient's body.
- Scenario 2: The parameters simulate 1 kg of the hypothetical mud distributed in a 2-D disk, with area of 2000 cm^2, which is 10% of the total body surface area of a male adult, simulating the situation when the mud is applied over one of the legs of the patient.

  In both scenarios, a total time of 100 h of mud application was assumed.

According to the procedure described in the ICRP Publication 103 (ICRP, 2007), the equivalent dose H_T was assessed by

$$H_T = \sum_R D_{T,R} \cdot w_R$$

where, H_T is the equivalent dose absorbed by tissue T, $D_{T,R}$ is the absorbed dose in tissue T by radiation type R and w_R is the radiation weighting factor, equal to 1 for both beta and gamma radiation. As the application involves exclusively the topic application on the skin, the effective dose E was assessed as

$$E = \sum_T w_T \cdot H_T$$

where, w_T is the tissue weighting factor, equal to 0.01 for the skin.

The absorbed dose rate and total dose are shown in Table 8. The effective dose due to both beta and gamma radiation on the skin, during the treatment time span of 100 h, was found to be about 0.5 μSv, for whole body application, and 4 μSv for application over 10% of the body's surface.

The final results for the effective dose to the member of the public, in both scenarios, were of the order of a few μSv, representing three orders of magnitude lower than the reference level of 1 mSv per year, for the members of the public. Therefore, the radiation dose to the public arising from the presently studied practice may be considered negligible, even assuming very conservative exposure scenarios.

4. Conclusions

Samples of *in natura* and matured Peruíbe Black Mud (PBM) used for therapeutic treatment in Peruíbe, Brazil, were analyzed in order to determine their physicochemical, mineralogical, elemental and radiological characteristics.

It was determined that the PBM is a type of material mainly composed of silt–clayey and sand fine size particles. Quartz is the main constituent mineral along with small amounts of muscovite, feldspar, gypsum, kaolinite, pyrite, halite and smectite: this material is also characterized by its low carbonate content. The matured mud, after treatment with sea water, shows gypsum and halite enrichment. Results also support the conclusion that most of the silica present in the PBM is inert, not dispersive in polar or non-polar medium and, in the amorphous form, with the presence of diatoms. However, although in much smaller amounts, PBM is also composed by minerals with high degree of dispersion in the polar medium.

It was verified that the mud has high moisture content, probably due to a high amount of fine particles having large surface area and, therefore, more hydration sites.

Both PBM forms showed pH, approximately, neutral as that observed in medicinal and pharmaceutical clays found in the literature. CEC values ranged from 26 to 33 meq/100 g, indicating that this mud has good adsorption capacity.

It was found that the elements Cl and Mg are enriched in matured form compared to the *in natura* form, probably, due to precipitation processes occurring by the seawater addition and the scavenging of some fine non mineral fraction, caused by the seawater exchange during the maturation process. Considering trace elements, the *in natura* and matured mud forms do not present significant differences in their concentrations. The PBM may be characterized by being enriched in the elements, Br, Cr, Sb, Se, and Zn and depleted in Ca, Rb, and Ta. The elements Ce, Co, Cr, Cs, Eu, Fe, La, Lu, Nd, Sc, Sm, Th, U, and Yb represent,

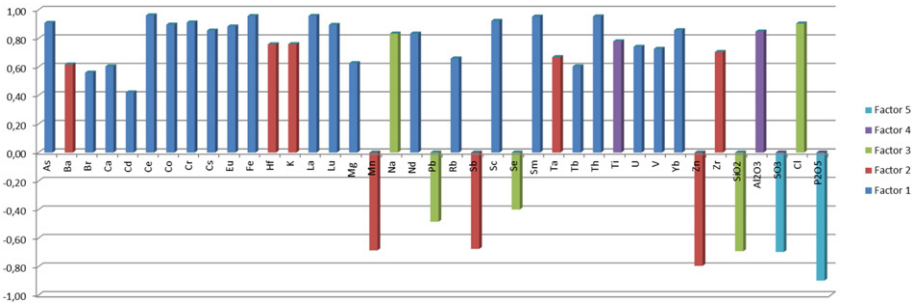

Fig. 6. Principal component analysis results obtained for the elemental distribution in the PBM samples.

Table 5
Carbon, hydrogen and nitrogen percentages, C/N and H/C ratios in the PBM samples.

Sample	C (%)	H (%)	N (%)	C/N	H/C
IN1	3.19	1.07	0.19	16.79	0.34
IN2	3.02	1.24	0.18	16.78	0.41
IN3	3.74	1.27	0.23	16.26	0.34
IN4	3.76	1.16	0.22	17.09	0.31
IN5	5.23	1.74	0.35	14.94	0.33
IN6	5.73	1.73	0.37	15.49	0.30
IN7	6.09	1.61	0.36	16.92	0.26
IN8	5.70	1.63	0.35	16.29	0.29
IN9	5.88	1.27	0.39	15.08	0.22
MAT1	3.93	1.34	0.15	26.20	0.34
MAT2	4.65	1.59	0.23	20.22	0.34
MAT3	4.57	1.55	0.17	26.88	0.34
MAT4	4.40	1.67	0.22	20.00	0.38
MAT5	5.28	1.68	0.28	18.86	0.32
MAT6	5.08	1.77	0.25	20.32	0.35
MAT7	3.01	0.80	0.12	25.08	0.27
MAT8	2.49	0.67	0.14	17.79	0.27
MAT9	3.47	0.93	0.17	20.41	0.27
MAT10	2.88	0.83	0.15	19.20	0.29

Table 6
The activity concentration obtained for ^{226}Ra, ^{228}Ra, ^{210}Pb and ^{40}K in the PBM samples in Bq kg^{-1}.

Sample	^{226}Ra	1σ	^{228}Ra	1σ	^{210}Pb	1σ	^{40}K	1σ
IN1	15.3	0.6	36.1	0.8	18	5	424	19
IN2	16.8	0.4	31.2	0.5	18	2	373	14
IN3	15.7	0.8	36	1	15	7	407	20
IN4	17.4	0.5	39.1	0.8	19	1	459	22
IN5	13.7	0.5	31	0.8	24	2	342	18
IN6	16.5	0.8	32.8	1	19	2	462	25
IN7	15.3	0.5	25.9	0.8	38	2	447	22
IN8	12.5	0.5	21.2	0.6	19	1	359	18
IN9	11	0.7	17.5	0.7	21	2	353	20
MAT1	15.2	0.5	33.5	0.8	20	2	445	22
MAT2	12.4	0.5	29.4	0.8	16	2	367	19
MAT3	18.4	0.7	37.8	0.9	32	6	454	20
MAT4	23.3	0.8	44.2	1.2	29	2	542	28
MAT5	12.6	0.6	22.3	0.7	28	2	403	21
MAT6	13	0.5	24.1	0.7	27	2	372	19
MAT7	15.2	0.5	28.5	0.7	26	2	417	21
MAT8	14.6	0.5	25.1	0.6	26	1	381	19
UNSCEAR (2010)	32		45 (^{232}Th)		33 (^{238}U)		420	

approximately, 56% of the variance observed in the samples and are those likely linked to the mineral structure by means of electrostatic interaction or bounded either to the amorphous iron and manganese oxy-hydroxides or to organic matter.

Considering the amount of potentially toxic elements available for skin exchange during the treatment, any harm supposed to occur to the patient arising from these elements is highly improbable.

Table 7
Input parameters for application of VARSKIN 3 code (Durham, 2006).

Parameter	Value
Source geometry	2-D disk
^{226}Ra	30 Bq
^{228}Ra	50 Bq
^{210}Pb	40 Bq
^{40}K	600 Bq
Skin density thickness	7 mg cm^{-2}
Air gap thickness	0 mm
Protective clothing thickness	0 mm
Protective clothing density	0 g cm^{-3}
Source diameter	According to the source area
Source area	2000 and 20,000 cm^2
Irradiation time	100 h
Irradiation area	2000 and 20,000 cm^2

Table 8
Absorbed dose results from VARSKIN 3 code (Durham, 2006).

Radiation type	Absorbed dose rate	Absorbed dose
Whole body application		
Beta	4.47×10^{-9} Gy/h	4.47×10^{-7} Gy
Gamma	8.32×10^{-7} Gy/h	8.32×10^{-9} Gy
Total	4.55×10^{-9} Gy/h	4.55×10^{-7} Gy
10% of the body's whole area application		
Beta	3.93×10^{-8} Gy/h	3.93×10^{-6} Gy
Gamma	6.68×10^{-6} Gy/h	6.68×10^{-4} Gy
Total	3.99×10^{-8} Gy/h	3.99×10^{-6} Gy

Radionuclides activity concentrations determined indicated that the PBM samples present, generally, lower values for the ^{238}U and ^{232}Th decay series members and have the same order of magnitude as that observed for ^{40}K, related to soils in general. The highest effective dose assessed was of the order of 4 μSv, considering a conservative exposure scenario, indicating that the therapeutic use of the mud poses no radiation risk to the individuals under therapeutic treatment.

Acknowledgments

Research supported under fellowship contract 2012/16642-9, by the São Paulo Research Foundation (Fundação de Amparo à Pesquisa do Estado de São Paulo — FAPESP), to whom the authors are grateful.

References

Abayazeed, S.D., El-Hinnawi, E., 2011. Characterization of Egyptian smectitic clay deposits by methylene blue adsorption. Am. J. Appl. Sci. 12, 1282–1286.
Al-Ashban, R.M., Aslam, M., Shah, A.H., 2004. A toxic traditional eye cosmetic study in Saudi Arabia. Publ. Health 118, 292–298.
Banin, A., Amiel, A., 1970. A correlative study of the chemical and physical properties of a group of natural soils of Israel. Geoderma 3, 185–198.
Britschka, Z.M.N., Teodoro, W.R., Velosa, A.P.P., Mello, S.B.V., 2007. The efficacy of Brazilian black mud treatment in chronic experimental arthritis. Rheumatol. Int. 28 (1), 39–45.
Cantaluppi, C., Fasson, A., Ceccotto, F., Cianchi, A., Degetto, S., 2014. Radionuclides concentration in water and mud of Euganean thermal district. Int. J. Environ. Res. 8 (1), 237–248.
Cara, S., Carcangiu, G., Padalino, G., Palomba, M., Tamanini, 2000. The bentonites in pelotherapy: chemical, mineralogical and technological properties of materials from Sardinia deposits (Italy). Appl. Clay Sci. 16, 117–124.
Carretero, M.I., Gomes, C.S.F., Tateo, F., 2006. Clays and human health. In: Bergaya, F., Theng, B.K.G., Lagaly, G. (Eds.), Handbook of Clay Science. Elsevier, Amsterdam, pp. 717–741.
Carretero, M.I., Pozo, M., Sánchez, C., García, F.J., Medina, J.A., Bernabé, J.M., 2007. Comparison of saponite and montmorillonite behaviour during static and stirring maturation with sea water for pelotherapy. Appl. Clay Sci. 36, 161–173.
Carretero, M.I., Pozo, M., Martín-Rubí, J.A., Pozo, E., Maraver, F., 2010. Mobility of elements in interaction between artificial sweat and peloids used in Spanish spas. Appl. Clay Sci. 48, 506–515.
Carretero, M.I., Gomes, C.S.F., Tateo, F., 2013. Clays, drugs, and human health. In: Bergaya, F.F., Lagaly, G. (Eds.), Developments in Clay Science 5. Elsevier, Amsterdam, pp. 711–764.
Carretero, M.I., Pozo, M., Legido, J.L., Fernández-González, M.V., Delgado, R., Gómez, I., Armijo, F., Maraver, F., 2014. Assessment of three Spanish clays for their use in pelotherapy. Appl. Clay Sci. 99, 131–143.
Churchman, G.J., Gates, W.P., Theng, B.K.G., Yuan, G., 2006. Clays and clay minerals for pollution control. In: Bergaya, F., Theng, B.K.G., Lagaly, G. (Eds.), Handbook of Clay Science. Elsevier, Armsterdam, pp. 625–675.
Currie, L.A., 2009. Nomenclature in evaluation of analytical methods including detection and quantification capabilities (IUPAC Recommendations 1995). Pure Appl. Chem. 67 (10), 1699–1723.
Cutshall, N.H., Larsen, L.H., Olsen, C.R., 1983. Direct analysis of ^{210}Pb in sediment samples: self-absorption corrections. Nucl. Instrum. Methods Res. 206, 309–312.
Dean, W.E., 1974. Determination of carbonate and organic matter in calcareous sediments and sedimentary rocks by loss on ignition: comparison with other methods. J. Sediment. Petrol. 44, 242–248.
Durham, J.S., 2006. "VARSKIN 3: A Computer Code for Assessing Skin Dose from Skin Contamination." NUREG/CR-6918. U.S. Nuclear Regulatory Commission, Washington, DC.
Einax, J.W., Zwanziger, H.W., Geib, S., 1997. Analytical chemistry: theoretical and metrological fundamentals. Chemometrics in Environmental Analysis. Wiley, Weinheim.
Fernández-González, M.V., Martín-García, J.M., Delgado, G., Párraga, J., Delgado, R., 2013. A study of the chemical, mineralogical and physicochemical properties of peloids prepared with two medicinal mineral waters from Lanjarón Spa (Granada, Spain). Appl. Clay Sci. 80–81, 107–116.

Filon, F.L., Maina, G., Adami, G., Venier, M., Coceani, N., Bussani, R., Massiccio, M., Barbieri, P., Spinelli, P., 2004. In vitro percutaneous absorption of cobalt. Int. Arch. Occup. Environ. Health 77, 85–89.
Foster, M.D., Survery, U.S.G., Washington, D.C., 1953. Geochemical studies of clay minerals: II — relation between ionic substitution and swelling in montmorillonites. Am. Mineral. 38, 994–1006.
Gemperline, P.J., 2006. Practical Guide to Chemometrics. 2nd ed. CRC Press, Boca Raton, FL.
Gomes, C., Carretero, M.I., Pozo, M., Maraver, F., Cantista, P., Armijo, F., Legido, J.L., Teixeira, F., Rautureau, M., Delgado, R., 2013. Peloids and pelotherapy: historical evolution, classification and glossary. Appl. Clay Sci. 75–76, 28–38.
IAEA – TECDOC – 564, 1990. Practical aspects of operating a neutron analysis laboratory. International Atomic Energy Agency, Vienna.
ICRP, 2007. The 2007 recommendations of the International Commission on Radiological Protection. ICRP Publ. 103, 2007.
Jang, K., Nunna, V.R.M., Hapugoda, S., Nguyen, A.V., Bruckard, W.J., 2014. Chemical and mineral transformation of a low grade goethite ore by dehydroxylation, reduction roasting and magnetic separation. Miner. Eng. 60, 14–22.
Karakaya, M.C., Karakaya, N., Sarıoğlan, S., Koral, M., 2010. Some properties of thermal muds of some spas in Turkey. Appl. Clay Sci. 48, 531–537.
Knorst-Fouran, A., Casás, L.M., Legido, J.L., Coussine, C., Bessières, D., Plantier, F., Lagière, J., Dubourg, K., 2012. Influence of dilution on the thermophysical properties of Dax peloid (TERDAX®). Thermochim. Acta 539 (10), 34–38.
López-Galindo, A., Viseras, C., 2004. Pharmaceutical and cosmetic applications of clays. In: Wypych, F., Satyanarayana, K.G. (Eds.), Clay Surfaces: Fundamentals and Applications. Elsevier, Armsterdam, pp. 267–289.
López-Galindo, A., Viseras, C., Cerezo, P., 2007. Compositional, technical and safety specifications of clays to be used as pharmaceutical and cosmetic products. Appl. Clay Sci. 36, 51–63.
MacDonald, D.D., Ingersoll, G., Berger, T.A., 2000. Development and evaluation of consensus-based sediment quality guidelines for freshwater ecosystems. Arch. Environ. Contam. Toxicol. 39, 20–31.
Medinsky, M.A., Cuddihy, R.G., McClellan, R.O., 1981. Systemic absorption of selenious acid and elemental selenium aerosols in rats. J. Toxicol. Environ. Health 8, 917–928.
Meyers, P.A., 2003. Applications of organic geochemistry to paleolimnological reconstructions: a summary of examples from the Laurentian Great Lakes. Org. Geochem. 34, 261–289.
Muñoz, M.S., Rodríguez, C.M., Rudnikas, A.G., Rizo, O.D., Martínez-Santos, M., Ruiz-Romera, E., Castillo, J.R.F., Pérez-Gramatges, A., Martínez-Villegas, N.V., Padilla, D.B., Díaz, R.H., González-Hernández, P., 2015. Physicochemical characterization, elemental speciation and hydrogeochemical modeling of river and peloid sediments used for therapeutic uses. Appl. Clay Sci. 104, 36–47.
Nikolov, J., Todorovic, N., Pantic, T.P., Forkapic, S., Mrdja, D., Bikit, I., Krmar, M., Veskovic, M., 2012. Exposure to radon in the radon spa Niška Banja, Serbia. Radiation Measurements, pp. 443–450.
Nordberg, F.G., Nogawa, K., Nordberg, M., Friberg, L.T., 2007. Cadmium. In: Nordberg, F.G., Fowler, B.A., Nordberg, M., Friberg, L.T. (Eds.), Handbook on the Toxicology of Metals. Elsevier, London, pp. 445–486.
Plumlee, G.S., Morman, S.A., Ziegler, T.L., 2006. The toxicological geochemistry of Earth materials: an overview of processes and the interdisciplinary methods used to understand them. In: Sahai, N., MAA, S. (Eds.), Medical Mineralogy and Geochemistry, Reviews in Mineralogy & Geochemistry 64, pp. 5–57.
Pozo, M., Carretero, M.I., Maraver, F., Pozo, E., Gómez, I., Armijo, F., Rubí, J.A.M., 2013. Composition and physico-chemical properties of peloids used in Spanish spas: a comparative study. Appl. Clay Sci. 83–84, 270–279.
Quintela, A., Terroso, D., Ferreira da Silva, E., Rocha, F., 2012. Certification and quality criteria of peloids used for therapeutic purposes. Clay Miner. 47, 441–451.
Ramasamy, V., Sundarrajan, M., Suresh, G., Paramasivam, K., Meenakshisundaram, V., 2014. Role of light and heavy minerals on natural radioactivity level of high background radiation area, Kerala, India. Appl. Radiat. Isot. 85, 1–10.
Roshchin, A.V., Taranenko, L.A., Murakova, N.Z., 1982. Sensitizing properties of indium, palladium and vanadium. Gig. Tr. Prof. Zabol. 2, 5–8.
Sánchez-Espejo, R., Aguzzi, C., Cerezo, P., Salcedo, I., López-Galindo, A., Viseras, C., 2014. Folk pharmceutical formulations in western Mediterranean: Identification and safety of clays used in pelotherapy. J. Ethnopharmacol. 155, 810–814.
Silva, P.S.C., Oliveira, S.M.B., Farias, L., Fávaro, D.I.T., Mazzilli, B.P., 2011. Chemical and radiological characterization of clay minerals used in pharmaceutics and cosmetics. Appl. Clay Sci. 52, 145–149.
Stauber, J.L., Florence, T.M., Gulson, B.L., Dale, L.S., 1994. Percutaneous absorption of inorganic lead compounds. Sci. Total Environ. 145, 55–70.
Talbot, M.R., Livingstone, D.A., 1989. Hydrogen index and carbon isotopes of lacustrine organic matter as lake level indicators. Palaeogeogr. Palaeoclimatol. Palaeoecol. 70, 121–137.
Tateo, F., Agnini, C., Carraro, A., Giannossi, M.L., Margiotta, S., Medici, L., Finizio, F.E., Summa, V., 2010. Short-term and long-term maturation of different clays for pelotherapy in an alkaline-sulphate mineral water (Rapolla, Italy). Appl. Clay Sci. 50, 503–511.
Taylor, S.R., McLennan, S.M., 1991. The continental crust: its composition and evolution. An examination of the geochemical record preserved in sedimentary rocks. Blackwell Scientific Publication, Carlton (312 pp.).
UNSCEAR (United Nations Scientific Committee on the Effects of Atomic Radiations), 2010f. UNSCEAR 2008 — sources and effects of ionizing radiation. Report to the General Assembly with Scientific Annexes I. United Nations, New York.
Veniale, F., Barberis, E., Carcangiu, G., Morandi, N., Setti, M., Tamanini, M., Tessier, D., 2004. Formulation of muds for pelotherapy: effects of "maturation" by different mineral waters. Appl. Clay Sci. 25, 135–148.
Vreca, P., Dolenec, T., 2005. Geochemical estimation of copper contamination in the healing mud from Makirina Bay, Central Adriatic. Environ. Int. 31, 53–61.
Wester, R.C., Maibach, H.I., Sedik, L., et al., 1993. In vivo and in vitro percutaneous absorption and skin decontamination of arsenic from water and soil. Fundam. Appl. Toxicol. 20, 336–340.
Wilson, G.P., Lamb, A.L., Leng, M.J., Gonzalez, S., Huddart, D., 2005. $\delta^{13}C$ and C/N as potential coastal palaeoenvironmental indicators in the Mersey Estuary, UK. Quat. Sci. Rev. 24, 2015–2029.